

Optimum DCT-Based Multicarrier Transceivers for Frequency-Selective Channels

Naofal Al-Dhahir, *Senior Member, IEEE*, Hlaing Minn, *Member, IEEE*, and Shilpa Satish

Abstract—We derive conditions on the impulse response and input signal of a frequency-selective finite-impulse response channel to be diagonalized by the discrete cosine transform (DCT) into parallel, decoupled, and memoryless subchannels. We show how these conditions can be satisfied in a practical multicarrier transceiver through a novel design of the guard sequence and the front-end prefilter. This DCT-based design results in complete elimination of interblock and intercarrier interference without channel knowledge at the transmitter and at the same guard sequence overhead, compared with DFT-based multicarrier transceivers. Extensions to multiinput multioutput frequency-selective channels are also described. Finally, we present numerical examples from wireline and wireless communications scenarios to illustrate the viability and practicality of the DCT as a modulation/demodulation basis for baseband and passband signaling over frequency-selective channels.

Index Terms—Discrete cosine transform (DCT), frequency-selective channel, guard sequence, multicarrier modulation (MCM), prefilter.

I. INTRODUCTION

MULTICARRIER modulation (MCM) [1] based on the discrete Fourier transform (DFT) has been adopted as the modulation/demodulation scheme of choice in several digital communications standards. These include wireline systems such as digital subscriber lines (DSL), where it is commonly known as discrete multitone (DMT), and wireless systems such as digital audio and terrestrial video broadcast (DAB/DVB-T), local area networks (IEEE 802.11a/g/n), and metropolitan area networks (IEEE802.16a), where it is commonly known as orthogonal frequency-division multiplexing (OFDM). In this paper, we shall refer to it generically by DFT-MCM.

DFT-MCM divides the frequency response of a finite-impulse response (FIR) frequency-selective channel into parallel, decoupled, and memoryless subchannels by adding a special guard sequence known as a *cyclic prefix* (CP) to each information block. This CP guard sequence (of length at least equal

to the channel memory) is chosen as a *periodic* extension of the information sequence, causing the linear convolution performed by the FIR channel to resemble a circular convolution. This renders the equivalent channel matrix *circulant*, and hence, perfectly diagonalizable by the DFT. Therefore, both interblock interference (IBI) between successive transmitted blocks and intercarrier interference (ICI) between the frequency subchannels in each block are eliminated. Additional attractive features of using the DFT orthogonal basis vectors for modulation/demodulation are efficient computation using the fast Fourier transform (FFT) algorithm and their independence of the channel characteristics. These two features are lost when using an all-zeros guard sequence (commonly known as *zero stuffing* [2]), since the optimum orthogonal modulation/demodulation basis vectors in this case are the eigenvectors of the channel matrix, which are both channel-dependent and computationally intense.

The only restrictions on the guard sequence are being redundant (i.e., it carries no new information) and having a length at least equal to the channel memory. As far as channel throughput is concerned, it was shown in [3] that, in each transmitted block, the guard sequence can be assumed a *linear deterministic* function of the information sequence without loss of optimality. This leads us to the following fundamental question: *Are there guard sequence designs (other than CP) that result in an equivalent channel matrix perfectly diagonalizable (i.e., no IBI and ICI) by an orthogonal channel-independent set of finite-dimensional modulation/demodulation vectors which have a fast implementation algorithm comparable to the FFT?* To the best of our knowledge, this question has not been addressed in the literature before.

In this paper, we show that the answer to the above question is affirmative by developing another MCM design that satisfies these desirable properties based on the discrete cosine transform (DCT) and a guard sequence that *symmetrically* extends the information sequence. In addition, our new design, referred to henceforth by DCT-MCM, has the following additional attractive features inherited from the DCT [4].

- The DCT basis is well known to have excellent spectral compaction and energy concentration properties. This, in turn, leads to improved performance with interpolation-based channel estimation [5] and can result in improved adaptive filtering convergence (see, e.g., [6, p. 584]).
- Recently, it was shown analytically in [7] that in the presence of frequency offset, the ICI coefficients in DCT-MCM are more concentrated around the main coefficient (i.e., less ICI leakage to adjacent subcarriers) than in DFT-MCM. This results in better performance robustness to frequency offsets.

Paper approved by G.-H. Im, the Editor for Equalization and Multicarrier Techniques of the IEEE Communications Society. Manuscript received November 16, 2004; revised July 22, 2005. The work of N. Al-Dhahir was supported in part by the Texas Advanced Technology Program (ATP) under Contract 009741-0023-2003, in part by the National Science Foundation under Contracts 04-30654 and 05-28010, and in part by matching funds from the Erik Jonsson School of Engineering, University of Texas at Dallas. This paper was presented in part at the IEEE Wireless Communications and Networking Conference, March 2005.

The authors are with the Department of Electrical Engineering, The University of Texas at Dallas, Richardson TX 75083 USA (e-mail: aldhahir@utdallas.edu).

Digital Object Identifier 10.1109/TCOMM.2006.873980

- The DCT is widely adopted in image/video coding standards (e.g., JPEG, MPEG, H.261). Using it for modulation/demodulation on frequency-selective channels results in a better integrated system design and a reduced overall implementation cost.
- The DCT uses only *real* arithmetic, as opposed to the complex-valued DFT. This reduces the signal-processing complexity/power consumption, especially for real pulse-amplitude modulation (PAM) signaling, where DFT-based processing still uses complex arithmetic and suffers from inphase/quadrature (I/Q) imbalance problems, which can cause appreciable performance degradation [8]. Furthermore, using DFT-MCM for baseband transmission systems such as DSL, the complex quadrature amplitude modulation (QAM) information block is constrained to be conjugate-symmetric to ensure a real-valued inverse DFT (IDFT) output at the transmitter. The same spectral efficiency at a lower receiver implementation complexity can be achieved with real (PAM) *unconstrained* information block and real-valued DCT-based receiver processing.¹

On the other hand, the main complexity disadvantage of DCT-MCM, compared with DFT-MCM, is the additional prefilter needed at the receiver to satisfy the symmetric channel impulse response (CIR) constraint for short channels. For long channels, DFT-MCM also requires a prefilter to shorten the channel.

In recent years, there have been intense research efforts aimed at designing multicarrier transceivers with better spectral containment properties (lower subchannel sidelobes) than the conventional DFT-MCM with a rectangular time window² to reduce the effect of narrowband interference (NBI) which leaks into adjacent subcarriers. Among those designs is the family of discrete wavelet multitone modulation (DWTMT); see, e.g., [10]–[12] and references therein. The main difference between DWTMT and our proposed DCT-MCM is that in the latter (using the proposed symmetric guard sequence and prefilter designs), we are able to achieve perfect diagonalization of the frequency-selective channel; i.e., there is no residual ICI or IBI, and hence, a simple one-tap per subchannel equalizer is optimum. This is unlike DWTMT schemes, where there is still residual ICI and IBI, and hence, more complex equalization is needed. In fact, DWTMT schemes use equalization both in time (as a tapped-delay line) and in frequency (a linear combiner across adjacent subchannels) to reduce IBI and ICI, as shown in [10] and [11]. Reducing the complexity of this time-frequency equalizer is investigated in [13]. Another important difference is that DWTMT schemes use block lengths longer than the FFT length (typically four times longer, as shown in [10]). This results in higher processing delay and complexity. The advantage of DWTMT is that, by properly designing the prototype FIR filters, we can achieve much lower subcarrier sidelobes, which results in higher immunity against NBI.

The main contribution of this paper is a novel design of a DCT-based MCM transceiver that optimally diagonalizes a fre-

quency-selective channel into parallel, decoupled, and memoryless subchannels. Critical to this diagonalization is the incorporation of a new symmetry constraint that we propose for the design of the FIR front-end prefilter. Furthermore, we generalize our DCT-MCM design to multiple-input multiple-output (MIMO) channels.

This paper is organized as follows. We start in Section II by describing the input–output block transmission model and stating our assumptions. In particular, we show analytically how different guard-sequence designs lead to different overall equivalent channel matrix representations. This is followed by a mathematical formulation of the DCT-MCM design problem. Section III contains the new contributions of this paper; namely, the DCT optimality conditions as modulation/demodulation vectors for frequency-selective channels, and our proposed guard sequence and prefilter designs to satisfy these conditions. Furthermore, we briefly describe the receiver signal detection algorithms in DCT-MCM, and we discuss generalizations to complex (passband) signaling and to MIMO channels. Numerical examples from DSL and wireless transmission scenarios are given in Section IV to illustrate our proposed designs, and the paper is concluded in Section V.

II. BACKGROUND

In this section, we start by describing our model for block transmission over a frequency-selective channel. Then, we show how the choice of the guard sequence affects the overall channel model. This is followed by a brief review of the DCT and a key diagonalization result.

A. Channel Model and Assumptions

We consider block-by-block transmission where the information symbols are divided into blocks, each of length N , and assume the standard discrete-time representation of a linear time-invariant³ frequency-selective channel, where the received symbols are given by

$$y_k = \sum_{m=-\nu}^{\nu} h_m x_{k-m} + z_k \quad (1)$$

where h_m is the m th coefficient of the *real-valued* CIR, which has a memory of 2ν . The information symbols $\{x_k\}$ are assumed zero-mean with an N -dimensional autocorrelation matrix $\mathbf{R}_{x,x}$. For simplicity, we shall first assume 1-D (PAM) signaling, where both the input symbols and the CIR are real-valued, but the results can be easily extended to the complex case, as will be shown in Section III-D. The additive white Gaussian noise (AWGN) symbols are denoted by $\{z_k\}$ and have variance σ_z^2 . Additional 2ν guard symbols are added before (ν prefix symbols) and after (ν suffix symbols) the information symbols to eliminate IBI at the expense of a throughput loss factor of $2\nu/(N + 2\nu)$. Furthermore, 2ν output symbols corresponding to the guard symbols are discarded at the receiver to eliminate their interfering effect. Over the

¹In this case, both the time-domain shortening filter and the frequency-domain one-tap equalizer are real-valued for DCT-MCM, while they are complex-valued for DFT-MCM.

²The subchannel sidelobes of DFT-MCM can be lowered significantly using more advanced windowing techniques, as described in detail in [9].

³The channel is assumed time-invariant over each transmission block but can vary from block to block.

remaining N output symbols, (1) can be expressed in matrix form as follows:

$$\begin{bmatrix} y_k \\ y_{k+1} \\ \vdots \\ y_{k+N-1} \end{bmatrix} = \begin{bmatrix} h_\nu & \cdots & h_0 & \cdots & h_{-\nu} & 0 & \cdots & 0 \\ 0 & h_\nu & \cdots & h_0 & \cdots & h_{-\nu} & 0 & \vdots \\ \vdots & \vdots & \ddots & \vdots & \ddots & \vdots & \ddots & 0 \\ 0 & \cdots & 0 & h_\nu & \cdots & h_0 & \cdots & h_{-\nu} \end{bmatrix} \times \begin{bmatrix} x_{k-\nu} \\ \vdots \\ x_{k-1} \\ x_k \\ \vdots \\ x_{k+N-1} \\ x_{k+N} \\ \vdots \\ x_{k+N+\nu-1} \end{bmatrix} + \begin{bmatrix} z_k \\ z_{k+1} \\ \vdots \\ z_{k+N-1} \end{bmatrix} \quad (2)$$

where $k = i(N + 2\nu) + \nu$ and $i = 0, 1, \dots$ is the block index. By partitioning the input vector into three components corresponding to the *prefix*, *suffix*, and *information* symbols, we can write (2) using compact matrix notation as follows:

$$\mathbf{y}_{k:k+N-1} = \mathbf{H} \mathbf{x}_{k-\nu:k+N+\nu-1} \mathbf{z}_{k:k+N-1} \quad (3)$$

$$= \mathbf{H}_{\text{pre}} \mathbf{x}_{k-\nu:k-1} + \mathbf{H}_{\text{info}} \mathbf{x}_{k:k+N-1} + \mathbf{H}_{\text{suf}} \mathbf{x}_{k+N:k+N+\nu-1} + \mathbf{z}_{k:k+N-1} \quad (4)$$

where bold capital and small letters are used to denote matrices and vectors, respectively. Furthermore, the subscripts of the vector denote the indexes of its first and last elements, separated by a colon. The corresponding partitioning of the channel matrix \mathbf{H} is defined by

$$\mathbf{H}_{\text{pre}} = \mathbf{H} \begin{bmatrix} \mathbf{I}_\nu \\ \mathbf{0}_{N \times \nu} \\ \mathbf{0}_{\nu \times \nu} \end{bmatrix} = \begin{bmatrix} h_\nu & \cdots & h_1 \\ 0 & \ddots & \vdots \\ \vdots & \ddots & h_\nu \\ 0 & \cdots & 0 \\ \vdots & \vdots & \vdots \\ 0 & \cdots & 0 \end{bmatrix} \quad (5)$$

$$\mathbf{H}_{\text{suf}} = \mathbf{H} \begin{bmatrix} \mathbf{0}_{\nu \times \nu} \\ \mathbf{0}_{N \times \nu} \\ \mathbf{I}_\nu \end{bmatrix} = \begin{bmatrix} 0 & \cdots & 0 \\ \vdots & \vdots & \vdots \\ 0 & \cdots & 0 \\ h_{-\nu} & \ddots & \vdots \\ \vdots & \ddots & 0 \\ h_{-1} & \cdots & h_{-\nu} \end{bmatrix}$$

$$\mathbf{H}_{\text{info}} = \mathbf{H} \begin{bmatrix} \mathbf{0}_{\nu \times N} \\ \mathbf{I}_N \\ \mathbf{0}_{\nu \times N} \end{bmatrix} = \begin{bmatrix} h_0 & \cdots & h_{-\nu} & 0 \\ \vdots & \ddots & \vdots & \vdots \\ h_\nu & & h_0 & h_{-\nu} \\ 0 & \ddots & \vdots & \vdots \\ 0 & h_\nu & \cdots & h_0 \end{bmatrix} \quad (6)$$

where \mathbf{I}_l denotes the identity matrix of size l and $\mathbf{0}_{m \times n}$ denotes the all-zeros matrix with m rows and n columns.

B. Guard Sequence

The two length- ν guard sequences do not carry new information, i.e., they are related by deterministic functions to the length- N information sequence $\mathbf{x}_{k:k+N-1}$. It was shown in [3] that assuming these functions to be *linear* does not limit the achievable channel throughput. Hence, we follow this assumption in this paper, i.e., we can write

$$\mathbf{x}_{k-\nu:k-1} = \mathbf{G}_{\text{pre}} \mathbf{x}_{k:k+N-1} \quad (7)$$

$$\mathbf{x}_{k+N:k+N+\nu-1} = \mathbf{G}_{\text{suf}} \mathbf{x}_{k:k+N-1} \quad (8)$$

where \mathbf{G}_{pre} and \mathbf{G}_{suf} are $\nu \times N$ fixed (independent of the channel) matrices that completely determine the guard sequences. Therefore, (4) becomes

$$\begin{aligned} \mathbf{y}_{k:k+N-1} &= (\mathbf{H}_{\text{info}} + \mathbf{H}_{\text{pre}} \mathbf{G}_{\text{pre}} + \mathbf{H}_{\text{suf}} \mathbf{G}_{\text{suf}}) \\ &\quad \times \mathbf{x}_{k:k+N-1} + \mathbf{z}_{k:k+N-1} \\ &= \mathbf{H}_{\text{eqv}} \mathbf{x}_{k:k+N-1} + \mathbf{z}_{k:k+N-1} \end{aligned} \quad (9)$$

where \mathbf{H}_{eqv} is the $N \times N$ equivalent channel matrix which is a function of the original CIR, \mathbf{G}_{pre} , and \mathbf{G}_{suf} . Equation (9) clearly shows how a different choice of the guard sequence results in a different overall channel matrix \mathbf{H}_{eqv} . For example, for DFT-MCM,⁴ the guard sequences are chosen as *cyclic extensions* of the information sequence; i.e., $\mathbf{G}_{\text{pre}} = [\mathbf{0}_{\nu \times (N-\nu)} \quad \mathbf{I}_\nu]$ and $\mathbf{G}_{\text{suf}} = [\mathbf{I}_\nu \quad \mathbf{0}_{\nu \times (N-\nu)}]$. It can be readily checked that \mathbf{H}_{eqv} becomes a *circulant* matrix, which is diagonalizable by the DFT.

C. Discrete Cosine Transform

There are eight types of DCT [14]. In this paper, we only consider the type-II DCT because it is the most popular in practice (used in JPEG, MPEG, and H.261 standards), and the first one discovered in [15]. The size- N type-II DCT is defined by the real orthogonal matrix whose (l, m) entry is given by

$$C(l, m) = \begin{cases} \sqrt{\frac{2}{N}} \cos\left(\frac{(l-1)(2m-1)\pi}{2N}\right), & 1 \leq l, m \leq N, l \neq 1 \\ \sqrt{\frac{1}{N}}, & l = 1. \end{cases}$$

It can be readily checked that $\mathbf{C}^t \mathbf{C} = \mathbf{C} \mathbf{C}^t = \mathbf{I}_N$ where $(\cdot)^t$ denotes the transpose.

We shall use the following key fact from [14, p. 2634] in designing our DCT-MCM transceiver.

Fact: All $N \times N$ matrices diagonalizable by the type-II DCT matrix can be written as the sum of an $N \times N$ *symmetric* Toeplitz matrix \mathbf{T} and an $N \times N$ *Hankel*⁵ matrix \mathbf{L} ; i.e., $\mathbf{C}(\mathbf{T} + \mathbf{L})\mathbf{C}^t = \mathbf{D}$ where \mathbf{D} is a diagonal matrix. Moreover, \mathbf{L} is determined from \mathbf{T} through the relations⁶

$$\begin{aligned} \mathbf{L} \mathbf{e}_1 &= \mathbf{S}_N \mathbf{T} \mathbf{e}_1 \\ \mathbf{L} \mathbf{e}_N &= \mathbf{J}_N \mathbf{L} \mathbf{e}_1 \end{aligned} \quad (10)$$

⁴Here, we assume that the DFT-MCM guard sequence is added as a CP and suffix for a direct comparison with DCT-MCM. It can also be added as a prefix only, which is more common in the DFT-MCM literature.

⁵A matrix is called Toeplitz if it is constant along the main diagonals, and called Hankel if it is constant along the main antidiagonals.

⁶These mathematical relations are not stated explicitly in [14], but can be inferred from the presentation.

where \mathbf{S}_k is the $k \times k$ upper-shift matrix (has ones on the first upper diagonal and zeros everywhere else), \mathbf{J}_k is the $k \times k$ reversal matrix (has ones on the main antidiagonal and zeros everywhere else), and \mathbf{e}_i is the i th unit vector (has a one in the i th position and zeros everywhere else). Note that since \mathbf{L} is a Hankel matrix, it is completely determined by its first and last columns, defined in (10). It is also important to note that this fact does not imply that all Toeplitz-plus-Hankel matrices are diagonalized by the type-II DCT, but only a subclass of them, where the Toeplitz matrix is symmetric and the Hankel matrix is related to it by (10). Henceforth, we shall refer to the type-II DCT by DCT only for brevity.

III. MAIN RESULTS

In this section, we address the fundamental question of this paper: *Can we design the guard sequences \mathbf{G}_{pre} and \mathbf{G}_{suf} so that \mathbf{H}_{eqv} is diagonalizable by the DCT?* We start with a mathematical formulation of the channel block throughput which is maximized by diagonalizing the equivalent channel matrix into decoupled subchannels, and optimally allocating input energy to these subchannels. This is followed by a precise statement of the conditions needed to achieve this diagonalization using the DCT. Then, we propose a practical design to satisfy these optimality conditions. Finally, the section is concluded by extending our design to MIMO and to passband transmission scenarios.

A. Channel Block Throughput

For the equivalent N -dimensional frequency-selective channel matrix with AWGN in (9), the channel block throughput, denoted by $I(\mathbf{X}; \mathbf{Y})$, for PAM signaling is given by⁷ [16]

$$I(\mathbf{X}; \mathbf{Y}) = \frac{1}{2} \frac{N}{N+2\nu} \log \det \left(\mathbf{I}_N + \frac{1}{\sigma_z^2} \mathbf{H}_{\text{eqv}}^t \mathbf{H}_{\text{eqv}} \mathbf{R}_{xx} \right) \quad (11)$$

$$= \frac{1}{2} \frac{N}{N+2\nu} \log \det \left(\mathbf{I}_N + \frac{1}{\sigma_z^2} \mathbf{C} \mathbf{H}_{\text{eqv}}^t \mathbf{H}_{\text{eqv}} \mathbf{C}^t \Sigma_x \right) \quad (12)$$

where $\det(\cdot)$ denotes the determinant of a matrix, and we used the matrix identity $\det(\mathbf{I} + \mathbf{A}\mathbf{B}) = \det(\mathbf{I} + \mathbf{B}\mathbf{A})$. Furthermore, since we are using the DCT basis for modulation, the input autocorrelation matrix admits the eigen-decomposition $\mathbf{R}_{xx} = \mathbf{C}^t \Sigma_x \mathbf{C}$.

It can be shown that the *channel block throughput is maximized when \mathbf{H}_{eqv} is diagonalized by the DCT*; i.e., $\mathbf{H}_{\text{eqv}} = \mathbf{C}^t \mathbf{D} \mathbf{C}$. In this case, (12) simplifies to

$$I(\mathbf{X}; \mathbf{Y}) = \frac{1}{2} \frac{N}{N+2\nu} \log \det \left(\mathbf{I}_N + \frac{1}{\sigma_z^2} \mathbf{D}^2 \Sigma_x \right) \quad (13)$$

⁷The factors of $1/2$ and $N/(N+2\nu)$ are due to 1-D (PAM) signaling and guard sequence overhead, respectively. We assume a basis of two for the logarithm, hence, $I(\mathbf{X}; \mathbf{Y})$ is measured in bits/block.

$$= \frac{1}{2} \frac{N}{N+2\nu} \sum_{i=1}^N \log \left(1 + \frac{d_i^2}{\sigma_z^2} \sigma_{x,i} \right) \quad (14)$$

where d_i and $\sigma_{x,i}$ denote the i th elements of the diagonal matrices \mathbf{D} and Σ_x , respectively. The optimum channel throughput is achieved by further optimizing the input energy-allocation profile $\sigma_{x,i}$ to maximize (14) subject to the average energy constraint

$$\begin{aligned} & \frac{1}{N+2\nu} \text{trace} \left(\mathbf{E} \left[\mathbf{x}_{k-\nu:k+N+\nu-1} \mathbf{x}_{k-\nu:k+N+\nu-1}^t \right] \right) = 1 \\ & \Rightarrow \text{trace} \left(\mathbf{E} \left[\begin{array}{c} \mathbf{G}_{\text{pre}} \mathbf{x}_{k:k+N-1} \\ \mathbf{x}_{k:k+N-1} \\ \mathbf{G}_{\text{suf}} \mathbf{x}_{k:k+N-1} \end{array} \right] \right. \\ & \quad \left. \times \left[\mathbf{x}_{k:k+N-1}^t \mathbf{G}_{\text{pre}}^t \mathbf{x}_{k:k+N-1}^t \mathbf{x}_{k:k+N-1}^t \mathbf{G}_{\text{suf}}^t \right] \right) \\ & = N + 2\nu \\ & \Rightarrow \text{trace}(\mathbf{R}_{xx}) + \text{trace}(\mathbf{G}_{\text{pre}} \mathbf{R}_{xx} \mathbf{G}_{\text{pre}}^t) \\ & \quad + \text{trace}(\mathbf{G}_{\text{suf}} \mathbf{R}_{xx} \mathbf{G}_{\text{suf}}^t) = N + 2\nu \\ & \Rightarrow \text{trace}(\Sigma_x) + \text{trace} \left(\Sigma_x \mathbf{C} \begin{bmatrix} \mathbf{I}_\nu & \mathbf{0} \\ \mathbf{0} & \mathbf{0} \end{bmatrix} \mathbf{C}^t \right) \\ & \quad + \text{trace} \left(\Sigma_x \mathbf{C} \begin{bmatrix} \mathbf{0} & \mathbf{0} \\ \mathbf{0} & \mathbf{I}_\nu \end{bmatrix} \mathbf{C}^t \right) = N + 2\nu \quad (15) \\ & \Rightarrow \sum_{i=1}^N \sigma_{x,i} \gamma_i = N + 2\nu \quad (16) \end{aligned}$$

where we used the relation $\text{trace}(\mathbf{A}\mathbf{B}) = \text{trace}(\mathbf{B}\mathbf{A})$ and the definition of \mathbf{G}_{pre} and \mathbf{G}_{suf} in (15). The constants γ_i in (16) can be precalculated as a function of the DCT matrix \mathbf{C} as follows (assuming $N \geq 2\nu + 1$, which is the case of interest, in practice, to avoid significant guard overhead):

$$\begin{aligned} \gamma_i &= 1 + \sum_{j=1}^{\nu} \mathbf{C}^2(i, j) + \sum_{j=N-\nu+1}^N \mathbf{C}^2(i, j), \quad 1 \leq i \leq N \\ &= 2 - \sum_{j=\nu+1}^{N-\nu} \mathbf{C}^2(i, j). \quad (17) \end{aligned}$$

The maximization of (14) subject to the constraint in (16) can be performed using standard Lagrange multiplier techniques, and will be illustrated by an example in Section IV.

B. DCT Optimality Conditions for Frequency-Selective Channels

For \mathbf{H}_{eqv} in (9) to be diagonalizable by the DCT, it must satisfy the conditions in (10). Note that \mathbf{H}_{info} becomes a symmetric Toeplitz matrix if and only if [see (6)]

$$h_i = h_{-i}, \quad i = 1, 2, \dots, \nu \quad (18)$$

which results in a symmetric linear-phase CIR. Then, it remains to choose \mathbf{G}_{pre} and \mathbf{G}_{suf} to make the matrix $\mathbf{H}_{\text{pre}}\mathbf{G}_{\text{pre}} + \mathbf{H}_{\text{suf}}\mathbf{G}_{\text{suf}}$ a Hankel matrix that satisfies (10) in addition to (18), i.e.,

$$\mathbf{H}_{\text{pre}}\mathbf{G}_{\text{pre}} + \mathbf{H}_{\text{suf}}\mathbf{G}_{\text{suf}} = \begin{bmatrix} h_1 & \cdots & h_\nu & 0 & \cdots & \cdots & 0 \\ \vdots & & 0 & \cdots & & & \vdots \\ h_\nu & 0 & \cdots & \ddots & & \ddots & \vdots \\ 0 & \cdots & \ddots & & \ddots & & 0 \\ \vdots & \ddots & & \ddots & & 0 & h_\nu \\ \vdots & & \ddots & & 0 & \vdots & \vdots \\ 0 & \cdots & \cdots & 0 & h_\nu & \cdots & h_1 \end{bmatrix}. \quad (19)$$

It can be easily checked that this condition is satisfied by setting

$$\mathbf{H}_{\text{pre}}\mathbf{G}_{\text{pre}} = \begin{bmatrix} h_1 & \cdots & h_\nu \\ \vdots & & \mathbf{0} \\ h_\nu & & \mathbf{0} \end{bmatrix} \Rightarrow \mathbf{G}_{\text{pre}} = \begin{bmatrix} \mathbf{J}_\nu & \mathbf{0}_{\nu \times (N-\nu)} \end{bmatrix} \quad (20)$$

$$\mathbf{H}_{\text{suf}}\mathbf{G}_{\text{suf}} = \begin{bmatrix} \mathbf{0} & & h_\nu \\ \mathbf{0} & & \vdots \\ h_\nu & \cdots & h_1 \end{bmatrix} \Rightarrow \mathbf{G}_{\text{suf}} = \begin{bmatrix} \mathbf{0}_{\nu \times (N-\nu)} & \mathbf{J}_\nu \end{bmatrix} \quad (21)$$

where we have used the definitions of \mathbf{H}_{pre} and \mathbf{H}_{suf} in (5) and (6), respectively. The expressions for \mathbf{G}_{pre} and \mathbf{G}_{suf} in (20) and (21) imply that

$$\begin{aligned} x_{k-i} &= x_{k+i-1}, & 1 \leq i \leq \nu \\ x_{k+N+i-1} &= x_{k+N-i}, & 1 \leq i \leq \nu. \end{aligned} \quad (22)$$

This reveals the design strategy for the prefix and suffix sequences: they should be chosen as *symmetric extensions* of the information sequence on both ends, with the axes of symmetry at the data-guard boundaries.

C. Receiver Signal Processing

1) *Front-End Prefilter*: The symmetry condition in (18) can be met, in practice, by implementing a FIR front-end prefilter, as follows.

- For channels with long memory, denoted by $L \geq (2\nu + 1)$, we propose to modify the design criterion for the FIR channel shortening prefilter commonly used in DFT-based multicarrier transceivers (see, e.g., [17]) by incorporating the symmetry constraint on the target (shortened) impulse response (TIR), as described briefly next. It was shown in [17] that the channel-shortening mean-square error (MSE) can be expressed in the following quadratic form:

$$\text{MSE} = \mathbf{h}^t \mathbf{R} \mathbf{h} \quad (23)$$

where $\mathbf{h} = [h_{-\nu} \cdots h_{-1} h_0 h_1 \cdots h_\nu]^t$ is the shortened CIR and \mathbf{R} is a positive-definite matrix that depends on the original CIR and the noise variance (see [17] for the exact

form of \mathbf{R}). We can impose the symmetry condition in (18) on \mathbf{h} by defining⁸

$$\mathbf{h} = \tilde{\mathbf{I}} \bar{\mathbf{h}} \quad (24)$$

where $\bar{\mathbf{h}} = [h_0 \cdots h_\nu]^t$ and the symmetric stacking matrix $\tilde{\mathbf{I}} = \begin{bmatrix} \mathbf{I}_{\nu+1} \\ \mathbf{J}_\nu \mathbf{0}_{\nu \times 1} \end{bmatrix}$. By combining (23) and (24), the prefilter design problem becomes

$$\text{Minimize MSE} = \bar{\mathbf{h}}^t \tilde{\mathbf{I}}^t \mathbf{R} \tilde{\mathbf{I}} \bar{\mathbf{h}} = \bar{\mathbf{h}}^t \bar{\mathbf{R}} \bar{\mathbf{h}}$$

subject to⁹ the unit-norm constraint $\bar{\mathbf{h}}^t \bar{\mathbf{h}} = 1$. The optimum $\bar{\mathbf{h}}$ is well known as the eigenvector of $\bar{\mathbf{R}} = \tilde{\mathbf{I}}^t \mathbf{R} \tilde{\mathbf{I}}$ corresponding to its minimum eigenvalue. The optimum symmetric shortened CIR is then calculated using (24) and the optimum prefilter coefficients are determined from the orthogonality principle of linear estimation [18] using the well-known Wiener equation (see [17] for details)

$$\mathbf{w} = \mathbf{R}_{yy}^{-1} \mathbf{R}_{yx} \mathbf{h} \quad (25)$$

where \mathbf{R}_{yx} and \mathbf{R}_{yy} are the output-input cross-correlation and the output autocorrelation matrices, respectively, which are calculated in closed form from the original channel matrix.

We emphasize that the symmetry constraint in (24) can also be incorporated into other prefilter designs based on criteria other than the minimum MSE (MMSE) criterion considered here, such as the maximum shortening SNR criterion described in [19].

- For channels with short memory (compared to block length N), we can still use the prefilter design algorithm described above by setting the original CIR length *equal* to the TIR length (i.e., no shortening), where the prefilter only equalizes the CIR to a symmetric one in a MSE sense. Alternatively, to reduce computational complexity, this prefilter can be set to the *time-reversed* (matched) filter to a memory- ν channel, resulting in an overall symmetric CIR with memory 2ν (see *Example 1* in Section IV). The price paid is a reduction in throughput from $N/N + \nu$ to $N/(N + 2\nu)$, which is still negligible for $N \gg \nu$.

In summary, satisfying the symmetric CIR condition in (18) can be achieved in practice using a FIR prefilter with computational complexity even less¹⁰ than its counterpart in DFT-MCM for long channels. For short channels, DFT-MCM does not require a prefilter, which is a complexity advantage over DCT-MCM. It is also worth mentioning that adding the symmetry condition makes the prefilter design more constrained in DCT-MCM, compared with DFT-MCM. Therefore, for a given number of prefilter taps, the achievable minimum shortening MSE will be higher for DCT-MCM. Alternatively,

⁸One of the reviewers kindly pointed out that a similar prefilter design method was proposed independently in [11].

⁹This constraint is introduced to avoid the trivial all-zeros solution.

¹⁰Because imposing the symmetry condition reduces the dimensionality of the prefilter optimization problem from $2\nu + 1$ to $\nu + 1$.

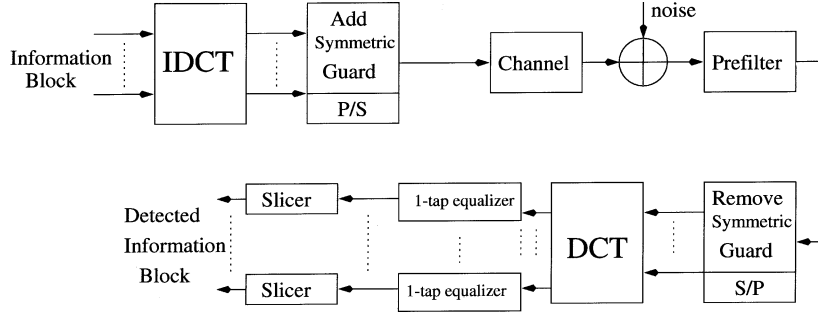


Fig. 1. DCT-MCM block diagram for baseband signaling.

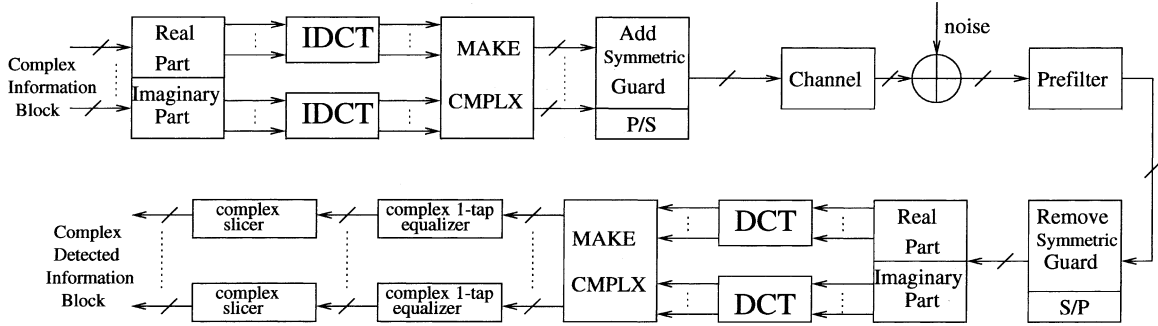


Fig. 2. DCT-MCM block diagram for passband signaling. Arrows with a strike indicate complex quantities. The block “MAKE CMLPX” generates a complex vector from two real vectors.

at a given shortening MSE, DCT-MCM will require a longer prefilter, which has a higher implementation complexity.

2) *Detection Algorithms*: By properly designing the guard sequence and the prefilter, conditions (18) and (22) are met. Then, starting from (9), we get

$$\mathbf{y}_{k:k+N-1} = \mathbf{H}_{\text{eqv}} \mathbf{x}_{k:k+N-1} + \mathbf{z}_{k:k+N-1} \quad (26)$$

$$= \mathbf{C}^t \mathbf{D} \mathbf{C} \mathbf{x}_{k:k+N-1} + \mathbf{z}_{k:k+N-1} \quad (27)$$

$$\Rightarrow \mathbf{Y}_{k:k+N-1} = \mathbf{C} \mathbf{y}_{k:k+N-1} \quad (28)$$

$$= \mathbf{D} \mathbf{X}_{k:k+N-1} + \mathbf{Z}_{k:k+N-1} \quad (29)$$

where capital letters denote the DCT-transformed quantities. Since \mathbf{D} is a real diagonal matrix, the components of $\mathbf{X}_{k:k+N-1}$ (the DCT transform of the information vector) are decoupled and can be individually detected by applying a simple zero-forcing (or MSE) scalar *real*¹¹ equalizer followed by a slicer. A block diagram of this DCT-based multicarrier transceiver architecture is shown in Fig. 1.

D. Complex Signaling

Our DCT-MCM transceiver design can be extended to the case of passband signaling, where both the input vector and the CIR are complex-valued, as shown in Fig. 2. Essentially, the optimality conditions in (18) and (22) are applied to the in-phase and quadrature dimensions. In other words, the complex guard sequence is set to be a symmetric extension of the complex information sequence in each transmitted block, and both the real and imaginary components of the complex baseband-equivalent CIR are constrained to be symmetric. The latter condition is

¹¹This is a complexity advantage over DFT-MCM, where this equalizer is complex even for real channels (as in DSL).

satisfied by implementing a complex front-end prefilter which shortens the CIR (if necessary, to fit the CP length) and makes both its real and imaginary components symmetric using the design criterion in (23) under the constraint in (24).

It is interesting to note here that, unlike the real case, using a time-reversed (matched) filter as a front-end prefilter in the complex case results in a conjugate-symmetric overall CIR, where only the real part is symmetric, whereas the imaginary part will be antisymmetric, and hence not diagonalizable by the type-II DCT.

Now, assuming that the guard sequence and the prefilter have been properly designed as described above, and starting from (26), we have

$$\begin{aligned} \mathbf{y}_{k:k+N-1} &= (\mathbf{H}_{\text{eqv}}^R + j\mathbf{H}_{\text{eqv}}^I) \mathbf{x}_{k:k+N-1} + \mathbf{z}_{k:k+N-1} \\ &\Rightarrow (\mathbf{y}_{k:k+N-1}^R + j\mathbf{y}_{k:k+N-1}^I) \\ &= (\mathbf{C}^t \mathbf{D}^R \mathbf{C} + j\mathbf{C}^t \mathbf{D}^I \mathbf{C}) \mathbf{x}_{k:k+N-1} + \mathbf{z}_{k:k+N-1} \\ &\Rightarrow \mathbf{Y}_{k:k+N-1} = \mathbf{C} (\mathbf{y}_{k:k+N-1}^R + j\mathbf{y}_{k:k+N-1}^I) \\ &= (\mathbf{D}^R + j\mathbf{D}^I) (\mathbf{X}_{k:k+N-1}^R + j\mathbf{X}_{k:k+N-1}^I) + \mathbf{Z}_{k:k+N-1} \\ &= \mathbf{D} \mathbf{X}_{k:k+N-1} + \mathbf{Z}_{k:k+N-1}. \end{aligned}$$

Since \mathbf{D} is a complex diagonal matrix, the complex information symbols are decoupled and can be individually detected by applying a complex scalar equalizer (one tap per subchannel), followed by a complex slicer, as shown in Fig. 2. The block “MAKE CMLPX” accepts two N -dimensional real vectors as inputs. Its output is an N -dimensional complex vector whose i th complex element is formed from the i th real elements of the two input vectors.

E. MIMO Channels

The DCT-MCM transceiver proposed in this paper can be applied to a system with n_i inputs and n_o outputs, by adding the symmetric prefix and suffix guard sequences to the length- N information blocks transmitted from each of the n_i inputs, and by imposing the symmetry condition on each of the resulting $n_i n_o$ CIRs when implementing the MIMO FIR prefilter of [20]. As in the single-input single-output (SISO) case described in Section III-C, we have to modify the design criterion of the prefilter in [20] to incorporate the symmetric TIR constraint by defining [c.f. (24)]

$$\mathbf{h} = \begin{bmatrix} \mathbf{I}_{n_o(\nu+1)} \\ \tilde{\mathbf{J}}_{n_o\nu} \mathbf{0}_{n_o\nu \times n_o} \end{bmatrix} \begin{bmatrix} \mathbf{h}_0 \\ \mathbf{h}_1 \\ \vdots \\ \mathbf{h}_\nu \end{bmatrix} \quad (30)$$

where each of the MIMO TIR coefficients \mathbf{h}_i is an $n_o \times n_i$ matrix and $\tilde{\mathbf{J}}_{n_o\nu}$ is a block reversal matrix (has the identity matrices \mathbf{I}_{n_o} on the main antidiagonal and zeros everywhere else).

To illustrate the DCT-based receiver signal processing in the MIMO case, consider for simplicity the case $n_i = n_o = 2$. Then, the input–output relationship in (26) generalizes to¹²

$$\begin{bmatrix} \mathbf{y}_1 \\ \mathbf{y}_2 \end{bmatrix} = \begin{bmatrix} \mathbf{H}_{\text{eqv}}^{1,1} & \mathbf{H}_{\text{eqv}}^{1,2} \\ \mathbf{H}_{\text{eqv}}^{2,1} & \mathbf{H}_{\text{eqv}}^{2,2} \end{bmatrix} \begin{bmatrix} \mathbf{x}_1 \\ \mathbf{x}_2 \end{bmatrix} + \begin{bmatrix} \mathbf{z}_1 \\ \mathbf{z}_2 \end{bmatrix} \quad (31)$$

$$= \begin{bmatrix} \mathbf{C}^t \mathbf{D}_{1,1} \mathbf{C} & \mathbf{C}^t \mathbf{D}_{1,2} \mathbf{C} \\ \mathbf{C}^t \mathbf{D}_{2,1} \mathbf{C} & \mathbf{C}^t \mathbf{D}_{2,2} \mathbf{C} \end{bmatrix} \begin{bmatrix} \mathbf{x}_1 \\ \mathbf{x}_2 \end{bmatrix} + \begin{bmatrix} \mathbf{z}_1 \\ \mathbf{z}_2 \end{bmatrix}. \quad (32)$$

Taking the length- N DCT of each of the received blocks, we have

$$\begin{bmatrix} \mathbf{Y}_1 \\ \mathbf{Y}_2 \end{bmatrix} = \begin{bmatrix} \mathbf{C} & \mathbf{0} \\ \mathbf{0} & \mathbf{C} \end{bmatrix} \begin{bmatrix} \mathbf{y}_1 \\ \mathbf{y}_2 \end{bmatrix} \quad (33)$$

$$= \begin{bmatrix} \mathbf{D}_{1,1} & \mathbf{D}_{1,2} \\ \mathbf{D}_{2,1} & \mathbf{D}_{2,2} \end{bmatrix} \begin{bmatrix} \mathbf{X}_1 \\ \mathbf{X}_2 \end{bmatrix} + \begin{bmatrix} \mathbf{Z}_1 \\ \mathbf{Z}_2 \end{bmatrix} \quad (34)$$

where capital letters denote DCT-transformed vectors. Now, we can apply standard multiuser detection algorithms [21] to (34) to jointly detect the k th subchannels of information blocks \mathbf{X}_1 and \mathbf{X}_2 . We conclude this section by emphasizing that this DCT-based approach can also be applied to MIMO systems that employ space–time coding (e.g., the Alamouti code [22]), and we omit the details here for brevity.

Remarks:

- 1) The throughput of the transmission scheme proposed in this paper is double that in [23], which is only $((N/2)/(N + 2\nu))$ since it restricts the information sequence to be symmetric as well. In contrast, our scheme only restricts the guard sequence (which is composed of redundant symbols anyway) to be a symmetric extension of the information sequence.
- 2) By adding the prefilter and designing the prefix and suffix guard sequences according to (22), we ensure optimality of the DCT for multicarrier transmission over frequency-selective channels in the sense that both ICI and IBI are completely eliminated.

¹²To simplify notation, we suppress the symbol time index in each vector, and use the subscript to denote the input–output index.

- 3) Analogous to single-carrier (SC) DFT-based complex equalizers [24], we can design an SC DCT-based real equalizer (by moving the IDCT operation to the receiver, before the slicer, in Fig. 1) and combine it with space–time block codes to realize both spatial and multipath diversity gains in a manner that parallels the DFT-based approach in [25].
- 4) The diagonal elements of \mathbf{D} in (29) which are key performance parameters [see (14)] are given by the (normalized) DCT transform of the first column of the equivalent channel matrix, i.e.,

$$d_i = \frac{\mathbf{e}_i^t \mathbf{C} \mathbf{H}_{\text{eqv}} \mathbf{e}_1}{\mathbf{e}_i^t \mathbf{C} \mathbf{e}_1}.$$

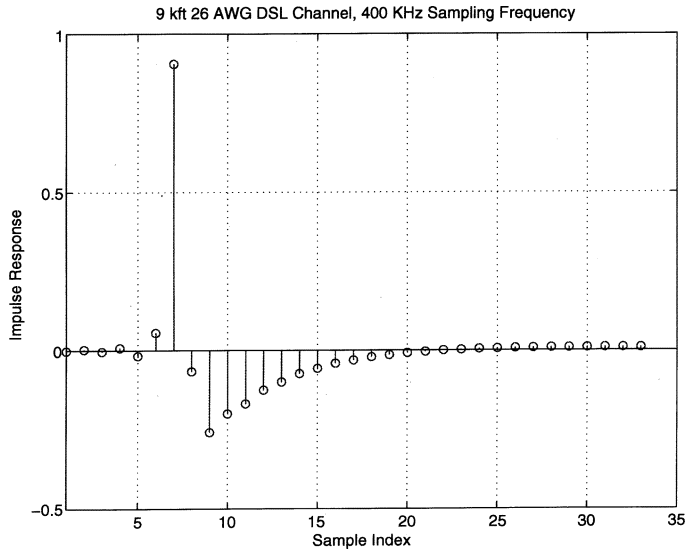
- 5) At high SNR, all subchannels are used and a flat input energy distribution ($\Sigma_{\mathbf{x}} = \mathbf{I}_N$) is near-optimum. Moreover, we can ignore the first term inside the determinant in (12), hence, the channel throughput is determined by $(\det(\mathbf{H}_{\text{eqv}}))^{2/N} = (\prod_{i=1}^N d_i^2)^{1/N}$, which is the *geometric average* of d_i^2 . For DFT-MCM, the corresponding performance measure is the geometric average of the squared magnitude of the channel's DFT coefficients [26]. These two measures are channel-dependent; hence, for some channels, DCT-MCM can outperform DFT-MCM (based on this measure), and vice versa. This observation has also been noted in terms of DCT- or DFT-based adaptive filtering performance, where convergence behavior depends on the statistics of the received signal [6].
- 6) It might be possible to use other DCT or discrete sine transform (DST) types [4], [14] as modulation/demodulation vectors for frequency-selective channels, but with their own symmetry (or antisymmetry) conditions on the CIR and the guard sequence. We do not pursue this further in this paper, since DCT-II is the most popular member of the DCT/DST family.

IV. NUMERICAL EXAMPLES

In this section, we present examples that illustrate the design of the front-end prefilter to achieve a symmetric CIR which can be diagonalized by the DCT after adding the symmetric guard sequence. We also present simulated performance comparisons between DFT-MCM and DCT-MCM in the presence of frequency offset.

Example 1 (Channel With Short Memory): Consider the two-tap channel with D -transform $1 + 0.9D$ (extensively studied in [27]) with block length $N = 16$ and input SNR of 10 dB. Since this CIR is not symmetric and $N \gg \nu$, we can implement the time-reversed front-end filter, resulting in the overall symmetric CIR $h(D) = (1 + 0.9D)(1 + 0.9D^{-1}) = 0.9D^{-1} + 1.81 + 0.9D$, where $\nu = 1$. With two guard symbols added symmetrically to each information block, we have an overall Toeplitz-plus-Hankel \mathbf{H}_{eqv} , which is diagonalized by the DCT to

$$\mathbf{D} = \text{diag}(3.61, 3.57, 3.47, 3.31, 3.08, 2.81, 2.50, 2.16, 1.81, 1.46, 1.12, 0.81, 0.54, 0.31, 0.15, 0.04).$$

Fig. 3. DSL CIR used in *Example 2*.

With a flat input energy distribution (i.e., $\sigma_{x,i} = 1$), we calculated the channel throughput using (14) to be 31.88 bits per block. To see the effect of input energy optimization on throughput, we calculated the constants γ_i in (17) to be

$$\gamma = \begin{bmatrix} 1.13 & 1.25 & 1.24 & 1.23 & 1.21 & 1.19 & 1.17 & 1.15 \\ 1.13 & 1.1 & 1.1 & 1.1 & 1.04 & 1.02 & 1.01 & 1.0 \end{bmatrix} \mathbf{1}.$$

Carrying out the input energy optimization procedure, we found that only 14 out of the available 16 subchannels should be allocated energy, as follows:

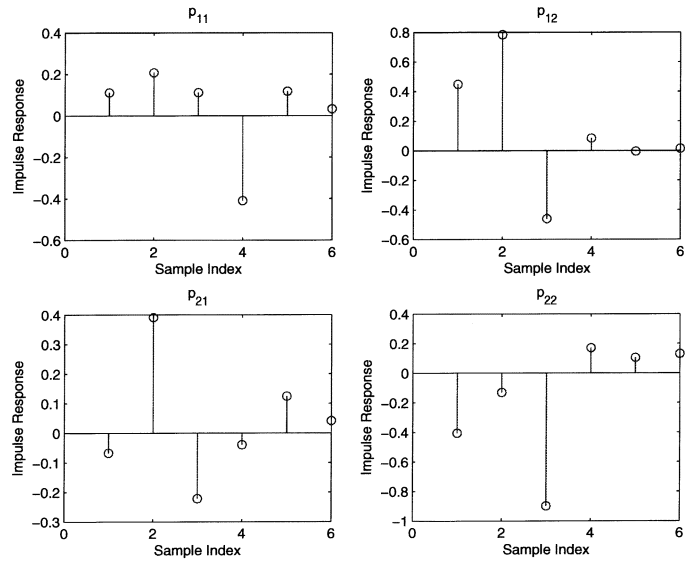
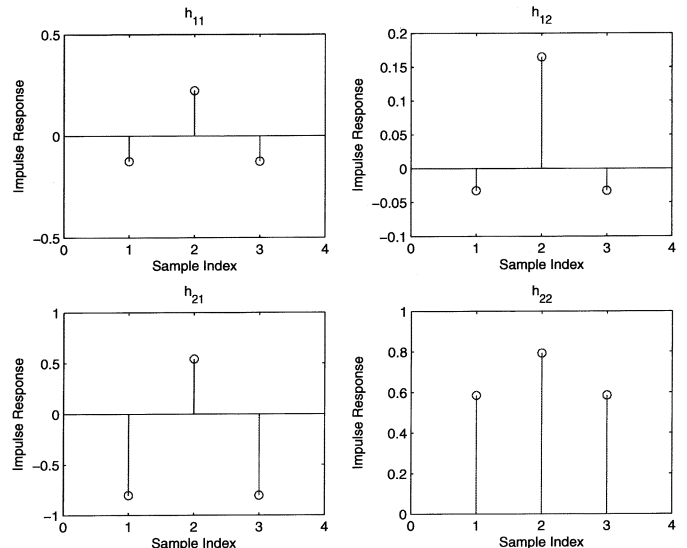
$$\Sigma_x = \text{diag}(1.25, 1.13, 1.13, 1.14, 1.16, 1.17, 1.19, 1.21, 1.23, 1.24, 1.24, 1.19, 1.02, 0.37, 0, 0)$$

and the resulting optimum channel throughput is 32.81 bits/block.

For scenarios where the CIR is short and nonsymmetric (as in this example), DCT-MCM is more complex than DFT-MCM, since the former requires a prefilter to make the overall CIR symmetric, which is not a requirement for the latter.

Example 2 (Channel With Long Memory): In this example, we illustrate the design of the front-end FIR prefilter to shorten nonsymmetric channels with long memory to short symmetric channels which are diagonalized by the DCT after adding the symmetric guard sequence. Consider a 9 kft 26 AWG DSL channel whose impulse response is depicted in Fig. 3 (has memory of 32 symbols). Assuming an input SNR of 20 dB, we designed (using the algorithm described in Section III-C) a 16-tap prefilter to shorten this DSL channel and found the optimum symmetric 3-tap CIR to be given by $\mathbf{h} = [-0.4144 \ 0.9101 \ -0.4144]^t$, which can now be diagonalized by the DCT.

Example 3 (MIMO Channels): Consider a 2×2 MIMO typical urban (TU) wireless channel with six symbol-spaced taps that have the power delay profile (PDP) (in decibels) $[-3 \ 0 \ -2 \ -6 \ -8 \ -10]$. A snapshot (single realization) of the four original CIRs, denoted by \mathbf{p}_{ij} for $1 \leq i, j \leq 2$ where each is a six-tap FIR filter, is given in Fig. 4. We assume quasi-static

Fig. 4. TU wireless MIMO CIR in *Example 3*.Fig. 5. Overall symmetric CIR in *Example 3* after prefiltering.

fading over the transmission blocks, and implement a 16-tap MIMO MMSE prefilter¹³ to simultaneously shorten the four FIR channels to symmetric three-tap ($\nu = 1$) channels. For an input SNR of 20 dB, we calculated the optimum symmetric TIRs to be (see Fig. 5)

$$\begin{aligned} \mathbf{h}_{11} &= [-0.1249 \ 0.2226 \ -0.1249] \\ \mathbf{h}_{12} &= [-0.0327 \ 0.1647 \ -0.0327] \\ \mathbf{h}_{21} &= [-0.8019 \ 0.5403 \ -0.8019] \\ \mathbf{h}_{22} &= [0.5853 \ 0.7933 \ 0.5853]. \end{aligned}$$

Example 4 (Complex Signaling): Here we consider Channel A, as specified in the wireless local area network (WLAN) ETSI

¹³We modified the identity norm constraint (INC) design criterion in [20] by incorporating the symmetry constraint on the TIR given in (30).

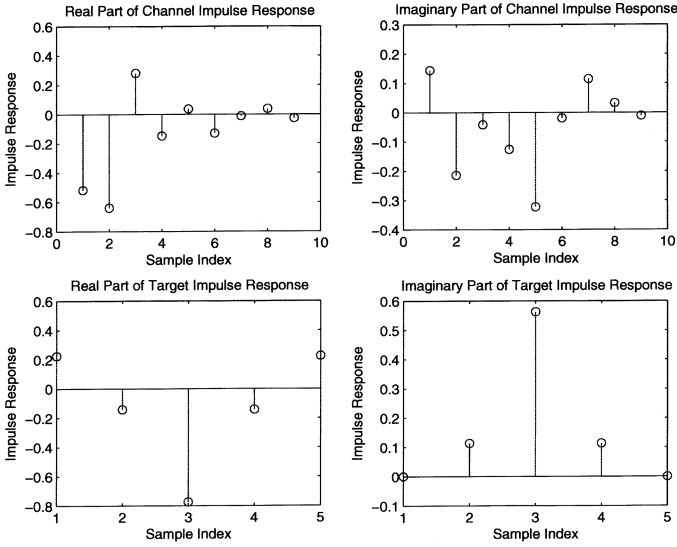


Fig. 6. Real and imaginary parts of the ETSI HIPERLAN2 channel A impulse response realization before and after filtering, as calculated in *Example 4*.

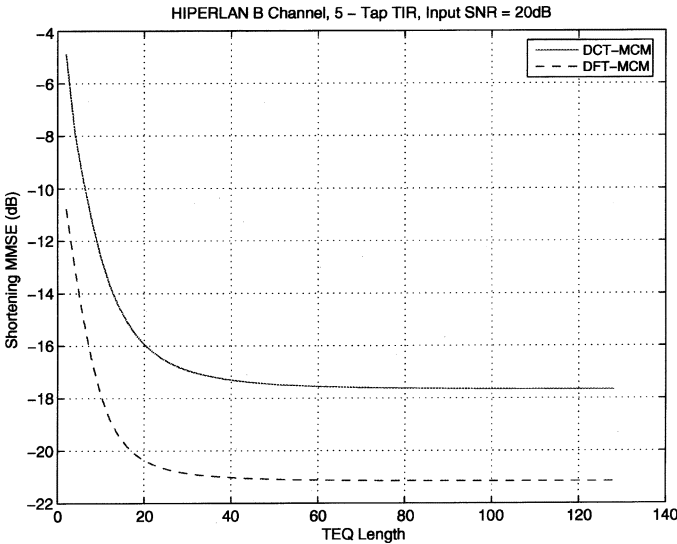


Fig. 7. Shortening MMSE (in decibels) versus prefilter length for DCT-MCM and DFT-MCM over HIPERLAN2 channel input SNR of 20 dB.

HIPERLAN2 standard [28], which models an office environment (no line of sight) with a maximum delay spread of 390 ns. The CIR has nine symbol-spaced channel taps and a PDP (in decibels) $[-1.73 \ -2.30 \ -4.46 \ -6.41 \ -9.96 \ -10.56 \ -12.72 \ -14.89 \ -17.10]$. A snapshot (single realization) of the real and imaginary parts of the baseband-equivalent complex CIR are shown in the top half of Fig. 6. Assuming an input SNR of 20 dB, we designed a complex 16-tap prefilter to shorten the complex CIR to a 5-tap ($\nu = 2$) complex impulse response with *symmetric* real and imaginary parts, as shown in the bottom half of Fig. 6. These two symmetric responses are then each diagonalized by the DCT into diagonal matrices \mathbf{D}^R and \mathbf{D}^I , as explained in Section III-D.

Example 5 (Frequency Offset): Finally, we compare the performance of DCT-MCM and DFT-MCM in the presence of frequency offset. We consider Channel B as specified in the wireless local area network (WLAN) ETSI HIPERLAN2 standard

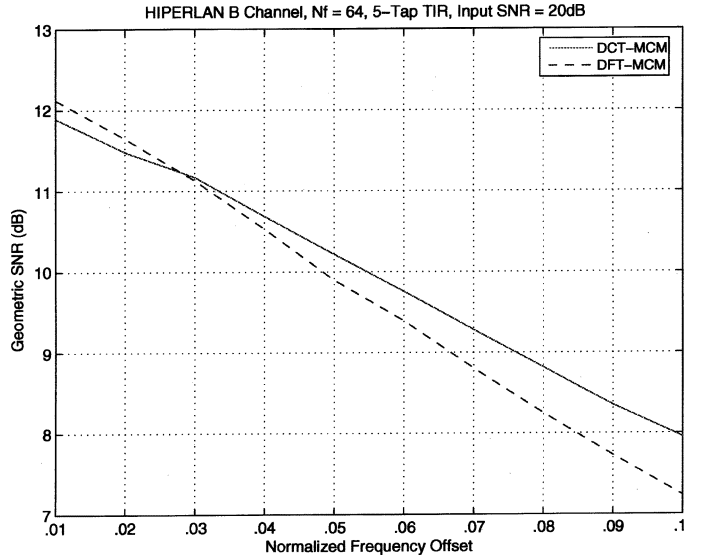


Fig. 8. Comparison of geometric SNR of DCT-MCM and DFT-MCM versus normalized frequency offset for HIPERLAN2 channel B and five-tap TIR at input SNR of 20 dB.

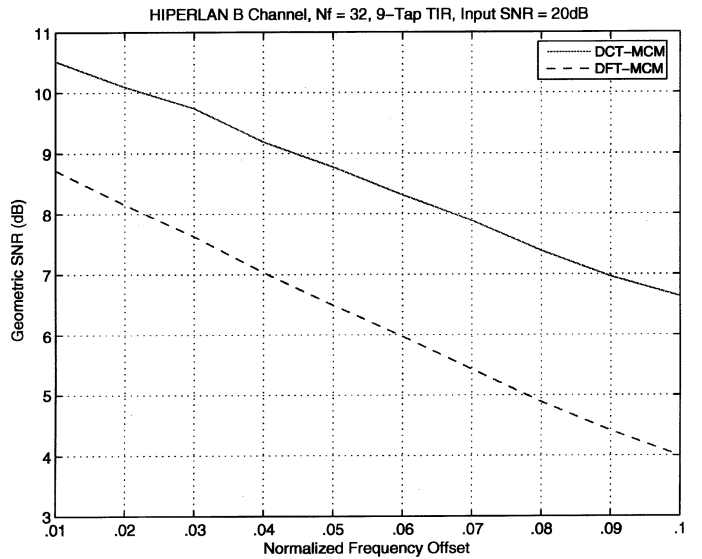


Fig. 9. Comparison of geometric SNR of DCT-MCM and DFT-MCM versus normalized frequency offset for HIPERLAN2 channel B and nine-tap TIR at input SNR of 20 dB.

[28], which models a highly dispersive office environment with a large maximum delay spread of 730 ns corresponding to a CIR with 16 symbol-spaced channel taps. Assuming an input SNR of 20 dB, we designed a prefilter to shorten the CIR to a 5-tap ($\nu = 2$) impulse response for both DFT-MCM and DCT-MCM. For the latter, the shortened channel was also constrained to be symmetric. Fig. 7 depicts the prefilter shortening MMSE (in decibels) versus its length, where it can be seen that 64 prefilter taps are sufficient to achieve the asymptotic MMSE. As expected, the asymptotic MMSE is higher for DCT-MCM because the prefilter is constrained to make the TIR symmetric, as well.

Figs. 8 and 9 compare the performance of DFT-MCM and DCT-MCM for $N = 128$ (as measured by the widely adopted

geometric SNR criterion [26]) averaged over 10 000 channel realizations for normalized (by the subchannel bandwidth) frequency offsets ranging from 0.01 to 0.1 and input SNR of 20 dB. It can be seen from the figures that DCT-MCM is more robust to frequency offset than DFT-MCM. This corroborates the analysis in [7], which showed that in the presence of frequency offset, the ICI coefficients of DCT-MCM are more concentrated around the main coefficient than in DFT-MCM, which results in less ICI leakage to adjacent subchannels.

Fig. 9 considers the scenario of a less-constrained prefilter where the TIR length is increased to nine taps ($\nu = 4$). We found that a prefilter length of 32 taps suffices in this case. Here, we can see that DCT-MCM outperforms DFT-MCM for the entire frequency-offset range under consideration. This is expected, because shortening the 16-tap channel to 9 taps is less demanding than shortening it to 5 taps. Hence, the DCT-MCM prefilter can do a better job at making the TIR symmetric.

V. CONCLUSIONS

The DCT is an optimal (in the sense of perfect channel diagonalization) modulation/demodulation basis for multicarrier signaling on FIR frequency-selective channels when the overall CIR is symmetric, and both the prefix and suffix guard sequences (of total length equal to the CIR memory) are symmetric extensions of the information sequence in each transmitted block. The first condition can be met by implementing a FIR prefilter, and the second condition is met by placing symmetry conditions only on the guard (not the information) sequence; hence, the guard overhead is identical to a DFT-MCM system. In addition, we showed how to further enhance the DCT-MCM transceiver performance by input energy optimization, and how to generalize it to complex signaling and to MIMO channels.

DCT-MCM has a comparable complexity to DFT-MCM for long channels, where both transceivers require a prefilter to limit the guard-sequence throughput overhead. For short channels, DCT-MCM still requires a prefilter (unlike DFT-MCM) which can be implemented as a simple time-reversed matched filter. Both DCT-MCM and DFT-MCM can perfectly diagonalize frequency-selective channels without requiring channel knowledge at the transmitter. Furthermore, our simulation results show that DCT-MCM is more robust to frequency offsets than DFT-MCM, in agreement with recent analytical results in [7].

In summary, our results in this paper show that DCT-MCM is a viable multicarrier transceiver which can be competitive with DFT-MCM in some practical scenarios. An interesting topic for future research is to perform more extensive performance comparisons between DFT-MCM and DCT-MCM under additional real-world channel impairments, such as in-phase/quadrature phase imbalance, timing offset, multipath spread longer than CP leading to IBI and ICI effects [29], NBI, channel-estimation errors, amplifier nonlinearities, and Doppler (mobility) conditions leading to additional IBI/ICI degradation.

REFERENCES

- [1] J. Bingham, "Multicarrier modulation for data transmission: An idea whose time has come," *IEEE Commun. Mag.*, pp. 5–14, May 1990.
- [2] S. Kasturia, J. Aslanis, and J. M. Cioffi, "Vector coding for partial-response channels," *IEEE Trans. Inf. Theory*, vol. 36, no. 4, pp. 741–762, Jul. 1990.
- [3] N. Al-Dhahir and S. N. Diggavi, "On the choice of guard sequence for block transmission over linear dispersive channels," *IEEE Trans. Commun.*, vol. 48, no. 6, pp. 938–946, Jun. 2000.
- [4] S. Martucci, "Symmetric convolution and the discrete sine and cosine transforms," *IEEE Trans. Signal Process.*, no. 5, pp. 1038–1051, May 1994.
- [5] Y. Yeh and S. Chen, "Efficient channel estimation based on discrete cosine transform," in *Proc. Int. Conf. Acoust., Speech, Signal Process.*, 2003, pp. 676–679.
- [6] A. H. Sayed, *Fundamentals of Adaptive Filtering*. New York: Wiley, 2003.
- [7] P. Tan and N. Beaulieu, "Precise bit error rate analysis of DCT OFDM in the presence of carrier frequency offset on AWGN channels," in *Proc. IEEE Globecom Conf.*, Nov. 2005, [CD-ROM].
- [8] J. Tubbx, B. Come, L. Perre, L. Deneire, S. Donnay, and M. Engels, "Compensation of IQ imbalance in OFDM systems," in *Proc. Int. Conf. Commun.*, 2003, pp. 3403–3407.
- [9] A. Redfern, "Receiver window design for multicarrier communication systems," *IEEE J. Sel. Areas Commun.*, vol. 20, no. 5, pp. 1029–1036, May 2002.
- [10] K. Cheong and J. Cioffi, "Discrete wavelet transform in multi-carrier modulation," in *Proc. IEEE Globecom*, Nov. 1998, pp. 2794–2799.
- [11] B. Boroujeny and Y. Chin, "Time domain equalizer for DWMT multicarrier transceivers," *IEE Electron. Lett.*, vol. 36, no. 18, pp. 1590–1592, Aug. 2000.
- [12] S. Sandberg and M. Tzannes, "Overlapped discrete multitone modulation for high-speed copper wire communications," *IEEE J. Sel. Areas Commun.*, vol. 13, no. 9, pp. 1571–1585, Dec. 1995.
- [13] B. Boroujeny, "Multicarrier modulation with blind detection capability using cosine modulated filter banks," *IEEE Trans. Commun.*, vol. 51, no. 12, pp. 2057–2070, Dec. 2003.
- [14] V. Sanchez, P. Garcia, A. Peinado, J. Segura, and A. Rubio, "Diagonalizing properties of the discrete cosine transform," *IEEE Trans. Signal Process.*, vol. 43, no. 11, pp. 2631–2641, Nov. 1995.
- [15] N. Ahmed, T. Natarajan, and K. Rao, "Discrete cosine transform," *IEEE Trans. Comput.*, vol. C-23, no. 1, pp. 90–93, Jan. 1974.
- [16] T. Cover and J. Thomas, *Elements of Information Theory*. New York: Wiley, 1991.
- [17] N. Al-Dhahir and J. M. Cioffi, "Efficiently computed reduced-parameter input-aided MMSE equalizers for ML detection: A unified approach," *IEEE Trans. Inf. Theory*, vol. 42, no. 5, pp. 903–915, May 1996.
- [18] T. Kailath, A. Sayed, and B. Hassibi, *Linear Estimation*. Englewood Cliffs, NJ: Prentice-Hall, 2000.
- [19] P. Melsa, R. Younce, and C. Rohrs, "Impulse response shortening for discrete multitone transceivers," *IEEE Trans. Commun.*, vol. 44, no. 12, pp. 1662–1672, Dec. 1996.
- [20] N. Al-Dhahir, "FIR channel-shortening equalizers for MIMO ISI channels," *IEEE Trans. Commun.*, vol. 50, no. 2, pp. 213–218, Feb. 2001.
- [21] S. Verdu, *Multuser Detection*. Cambridge, U.K.: Cambridge Univ. Press, 1998.
- [22] S. Alamouti, "A simple transmit diversity technique for wireless communications," *IEEE J. Sel. Areas Commun.*, vol. 16, no. 10, pp. 1451–1458, Oct. 1998.
- [23] G. Mandyam, "On the discrete cosine transform and OFDM systems," in *Proc. Int. Conf. Acoust., Speech, Signal Process.*, 2003, pp. 544–547.
- [24] H. Sari, G. Karam, and I. Jeanclaude, "Transmission techniques for digital terrestrial TV broadcasting," *IEEE Commun. Mag.*, pp. 100–109, Feb. 1995.
- [25] N. Al-Dhahir, "Single-carrier frequency-domain equalization for space-time block-coded transmissions over frequency-selective fading channels," *IEEE Commun. Lett.*, vol. 5, no. 7, pp. 304–306, Jul. 2001.
- [26] J. M. Cioffi, "A multicarrier primer," in *ANSI T1E1.4 Committee Contribution*, no. 91-157. Boca Raton, FL: CRC Press, Nov. 1991 [Online]. Available: <http://www.stanford.edu/group/cioffi/pdf/multicarrier.pdf>
- [27] —, *Class Notes for EE379*. Stanford, CA: Stanford Univ., 1998.
- [28] *Channel Models for HIPERLAN/2 In Different Indoor Scenarios*, Doc. 3ER1085B, ETSI Normalization Committee, 1998.
- [29] J. Seonae, S. K. Wilson, and S. Gelfand, "Analysis of intertone and interblock interference in OFDM when the length of the cyclic prefix is shorter than the length of the impulse response of the channel," in *Proc. Global Telecommun. Conf.*, 1997, vol. 1, pp. 32–36.



Naofal Al-Dhahir (S'89–M'90–SM'98) received the M.S. and Ph.D. degrees from Stanford University, Stanford, CA, in 1990 and 1994, respectively, both in electrical engineering.

He was an Instructor with Stanford University in 1993. From 1994 to 2003, he was a Principal Member of Technical Staff with the R&D Centers of GE and AT&T. Since August 2003, he has been an Associate Professor at the University of Texas at Dallas, Richardson. His current research interests include space–time coding and signal processing,

OFDM, wireless networks, and digital subscriber line technology. He has authored over 140 journal and conference papers and holds 16 U.S. patents. He is co-author of the book *Doppler Applications for LEO Satellite Systems* (New York: Springer, 2002).

Dr. Al-Dhahir is a member of the IEEE SP4COM and SPTM technical committees. He served as Editor for IEEE TRANSACTIONS ON SIGNAL PROCESSING and IEEE COMMUNICATIONS LETTERS, and is currently an Editor for IEEE TRANSACTIONS ON COMMUNICATIONS. He served as co-chair of the Communication Theory Symposium at Globecom'04. He received the best paper award at the IEEE VTC Fall'05 conference and the 2006 Donald G. Fink Best IEEE paper award.



Hlaing Minn (S'99–M'01) received the B.E. degree in electronics from Yangon Institute of Technology, Yangon, Myanmar, in 1995, the M.Eng. degree in telecommunications from the Asian Institute of Technology (AIT), Bangkok, Thailand, in 1997, and Ph.D. degree in electrical engineering from the University of Victoria, Victoria, BC, Canada, in 2001.

He was with the Telecommunications Program in AIT as a Laboratory Supervisor during 1998. He was a Research Assistant from 1999 to 2001 and a Post-

doctoral Research Fellow during 2002 in the Department of Electrical and Computer Engineering, University of Victoria. Since September 2002, he has been with the Erik Jonsson School of Engineering and Computer Science, University of Texas at Dallas, Richardson, TX, as an Assistant Professor. His research interests include wireless communications, statistical signal processing, error control, detection, estimation, synchronization, signal design, and cross-layer design.

Dr. Minn is an Editor for the IEEE TRANSACTIONS ON COMMUNICATIONS.



Shilpa Satish received the B.S. degree in electronics and communications from Viswesvariah Technological University, Bangalore, India, in 2003. She is currently working toward the M.S. degree in electrical engineering at the University of Texas at Dallas, Richardson.

After graduation, she worked for a year as a Network Engineer with Larson and Toubro InfoTech. Her main area of research is multicarrier modulation systems. Her research interests also include WiFi, WiMax standards and wireless/wire-

line networking protocols.